Published in : Journal of Molecular Structure (2020), vol. 1206, 127773
DOI:10.1016/j.molstruc.2020.127773
Status : Postprint (Author's version)

Structural and optical characterization of nitrogen and gallium codoped ZnO thin films, deposited by sol-gel method

T. Ivanova[a,*], A. Harizanova[a], T. Koutzarova[b], B. Vertruyen[c], R. Closset[c]

[a] *Central Laboratory of Solar Energy and New Energy Sources, Bulgarian Academy of Sciences, Tzarigradsko Chaussee 72, 1784, Sofia, Bulgaria*
[b] *Institute of Electronics, Bulgarian Academy of Sciences, Tzarigradsko Chaussee 72, 1784, Sofia, Bulgaria*
[c] *GREENMAT, Institute of Chemistry B6, University of Liege, B6a Quartier Agora, Allee Du Six Août, 13, 4000, Liège, Belgium*
[*] *Corresponding author. E-mail address: tativan@phys.bas.bg (T. Ivanova)*

KEYWORDS: Co-doped ZnO films, Sol-gel processing, Film morphology, Structure.

ABSTRACT

Nitrogen and gallium co-doped ZnO films have been successfully obtained by a sol-gel technology using spin coating. ZnO:N, ZnO:Ga and co-doped (N, Ga) ZnO films are deposited on silicon and quartz substrates. The structural, morphological and optical properties of ZnO:N:Ga thin films are studied depending on the thermal treatments (300–600 °C) and the two dopants: N and Ga. The investigations of the doped ZnO films have been performed by using X-ray Diffraction (XRD), Fourier Transform Infrared spectroscopy (FTIR), Field Emission Scanning Electron microscope (FESEM) and UVeVISeNIR spectrophotometry. It has been found that the co-doped (N, Ga) ZnO films are crystallized in the wurtzite structure with no impurity phases. The optical transparency of ZnO:Ga and ZnO:N:Ga films is above 80% in the spectral range of 400–800 nm, revealing a significant improvement compared to undoped ZnO films. Gallium and nitrogen co-doping in ZnO results in the modification of the surface morphologies changing from wrinkle-like (undoped ZnO) to closed packed grained microstructure (ZnO:N:Ga films).

Published in : Journal of Molecular Structure (2020), vol. 1206, 127773
DOI:10.1016/j.molstruc.2020.127773
Status : Postprint (Author's version)

1. Introduction

ZnO based materials are getting a huge research interest due to their potential applications in electronic, optoelectronic and sensing devices, ultraviolet light-emitting and laser diodes [1,2]. Zinc oxide is a promising candidate due to its chemical, optical and electrical properties such as wide band gap, large exciton energy, low cost, chemical stability, no toxicity etc. [3,4]. The modification of ZnO films to achieve desirable morphological, optical and electronic properties through impurity incorporation is currently an important approach for future applications [5].

Moreover, the undoped and doped ZnO films are suitable and attractive for applications in solar cells, photoelectrochemical cells (PECs), thin film transistors, nanogenerators, sensors, liquid crystal applications and other optoelectronic devices. Gallium is found to be a beneficial substitutional doping element because of similar ionic radii of Ga^{+} (0.062 nm) and Zn^{+} (0.072 nm), and the covalent bond lengths of Ga–O and Zn–O are very closed (1.92 and 1.97 Å, respectively), which can create a small deformation of ZnO crystal lattice even in the case of high Ga doping concentrations [6].

Another advantage of gallium over the other dopants is the fact that it is more moisture resistant and stable in oxidizing environments. Ga incorporation in ZnO films is manifested by improved optical transparency, low resistivity, enhanced sensitivity to UV light [7].

Nitrogen (N) is considered as the most appropriate dopant in ZnO lattice to substitute oxygen due to its high electronegativity and ionic radius similar to oxygen. Nitrogen incorporation is recognized as efficient approach for the realization of p-type doping in ZnO [8,9]. ZnO:N films are studied as photoelectrodes in photoelectrochemical cell for water splitting, p-type transperant conductors, ferromagnetic material, visible light photocatalyst [10,11]. As the solubility of nitrogen in ZnO is low, therefore, it is necessary to find ways to enhance its solubility limit [12,13]. It is well known that when two kinds of dopants with opposite effective charges are added to a matrix, the solubility limit of the dopants can be extended by their co-doping effect [14]. Many authors reported that the presence of gallium enhances the incorporation of nitrogen in ZnO matrix [15,16].

Sol-gel method is known to be a relatively simple and low cost route for obtaing high quality films and offering homogeneous dispersion of dopants [17]. The advantages of the sol-gel technology over other deposition methods include good composition control ability, easy approaches of film thickness and composition modification, large area coating capability, reproducibility versatility, and good film adhesion [18].

In this work, the sol-gel technology for preparation of nitrogen doped ZnO, gallium doped ZnO and N, Ga co-doped ZnO nanocomposite films is presented. The sol-gel derived (N, Ga) ZnO films are successfully obtained on quartz and silicon substrates by the spin coating method. The concentration of the dopants is changed. The obtained films are subjected to high temperature

Published in : Journal of Molecular Structure (2020), vol. 1206, 127773
DOI:10.1016/j.molstruc.2020.127773
Status : Postprint (Author's version)

treatments (300–600 °C). The study of the structural, optical and morphological properties of co-doped ZnO with undoped ZnO, ZnO:N and ZnO:Ga films is performed.

2. Experimental

Gallium and nitrogen co-doped ZnO films are deposited from N doped Zn solution and Ga doped solution by mixing in different molar ratios. All the chemical reagents used are analytical grade purity. The 0.4 M sol solution for ZnO deposition is synthesized by using zinc acetate dihydrate $Zn(CH_3COO)_2$ as a precursor, dissolved in absolute ethanol (Merck). The complexing agent is monoethanolamine (MEA) with a molar ratio MEA/Zn = 1. The detailed preparation procedure is described previously [19]. The Zn–Ga sol is obtained by dissolving 4 wt% $Ga(NO_3)xH_2O$ into Zn sol solution. The second sol (Zn–N) is derived by adding 1 wt% ammonium acetate (CH_3COONH_4) into the corresponding Zn sol solution. The mixed sols are prepared in the following procedure: equal amount of Zn–N sol is added to different quantities of Zn–Ga sol as described in **Table 1**.

Table 1. Description of sol solutions, used for depositing ZnO:N:Ga films.

	Zn–N solution (with 1 wt% CH_3COONH_4)	Zn-Ga solution (with 4 wt% $Ga(NO_3)xH_2O$)
Sol 1	5 ml	10 ml
Sol 2	5 ml	5 ml
Sol 3	5 ml	0.5 ml

The mixed sols are stirred on a magnetic stirrer at 50 °C for 2 h in order to get homogeneous solution with appropriate film forming properties. The sols go through ultrasonic treatment at 40 °C for 3 h. The prepared sol solutions are clear, transparent with no precipitations.

N and Ga co-doped ZnO films have been deposited by the spin coating method at 4000 rpm/30 s. The substrates are prelimanary cleaned. Silicon wafers are used for vibrational, structural and morphological studies and the quartz substrates for optical characterization. The films have been preheated at 300 °C/10 min. The coating and preheating treatment procedures are repeated five times to get thicker films. The sol-gel ZnO:N:Ga films are treated at temperatures 300, 400, 500 and 600 °C for 1 h in air ambient by using constant heating and cooling rates of 10 °C/min. This technological process permits to deposit uniform and homogeneous thin films. Undoped ZnO, ZnO:Ga and ZnO:N films are deposited from the corresponding sol solutions, following by similar technological procedures for comparison purposes.

X-Ray diffraction (XRD) patterns are recorded by XRD diffractometer Bruker D8 using a Cu anode ($\lambda_{K\alpha}$ = 1.54056 °A), and a grazing angle 2°, step time 8 s. Fourier transform infrared (FTIR) measurements are done by Shimadzu FTIR Spectrophotometer IRPrestige-21 in the spectral range 350–4000 cm^{-1}. The studied samples have been deposited on Si substrates and bare Si wafer (p-Si, with orientation <100>) is used as background. Optical measurements are carried out by UV–VIS–

Published in : Journal of Molecular Structure (2020), vol. 1206, 127773
DOI:10.1016/j.molstruc.2020.127773
Status : Postprint (Author's version)

NIR Shimadzu 3600 double-beam spectrophotometer in the spectral region of 240–1800 nm. The transmittance spectra are performed against air and the reflectance spectra are measured by using the specular reflectance attachment (for 5° incidence angle) and Al coated mirror as reference. The morphology of the sol-gel films is studied by FESEM microscopy (Philips XL 30FEG-ESEM, FEI).

3. Results and discussion

Fig. 1 presents XRD patterns of the sol-gel N doped, Ga doped and (N, Ga) co-doped ZnO films, treated at the temperatures ranging from 300 to 600 °C. The registered diffraction peaks could be indexed to the hexagonal wurtzite structure of zinc oxide with space group P63mc (186) (JCPDS card 01-070-8070). Previous study [20] reveals that the undoped sol-gel ZnO films are polycrystalline and the film crystallization is significantly enhanced with increasing the annealing temperature. The diffraction peaks of ZnO:Ga films reveal lower intensities, indicating that Ga addition causes a crystallinity deterioration. This effect has been previously found out for the sol-gel ZnO:Ga films with lower gallium concentrations [19], than those used in this study. XRD patterns (peak intensities and shapes) of ZnO:Ga films are not considerably influenced by the thermal treatments up to 500 °C. A certain enhancement of ZnO:Ga film crystallization can be observed after the highest temperature annealing at 600 °C. It is proved, that Ga doping in ZnO induces an worsening of the film crystallization as well as a decreasing of the crystallite sizes compared to undoped ZnO films [19]. No Ga and Ga containing phases are found, suggesting that Ga^{3+} have successfully substituted Zn^{2+} ions in ZnO lattice without secondary phase formation.

The crystalline structure of the nitrogen doped ZnO films manifest a strong dependence on the thermal treatments. The increase of the annealing temperatures leads to stronger and sharper XRD lines, a sign for higher crystallization. The nitrogen doping provokes an improvement of the film crystalization and the crystallite sizes grow greater compared to undoped ZnO films. It can also be observed a shift of the (002) peak to the higher angle (for 600 °C annealed films, see **Fig. 2**). The slightly larger 2 theta values may arise from the smaller bond length of Zn–N (1.88 Å) than that of Zn–O (1.93 Å). This fact can suppose that nitrogen has been successfully incorporated into zinc oxide lattice and N is partly substituted oxygen [21]. XRD analysis shows that ZnO:N films maintain the wurtzite phase of ZnO.

XRD investigation of ZnO:N:Ga films, treated at the temperatures 300–600 °C reveals that the studied films are polycrystalline in nature and XRD lines can be attributed only to wurtzite phase. The annealing procedures produce a small impact on the XRD patterns of ZnO:N:Ga films, obtained from the sol 1 and sol 2. The thermal treatments influences in a greater extent the crystallization behaviour of ZnO:N:Ga, sol 3 films. The crystallization of ZnO:N:Ga films has diminished comparing to ZnO and ZnO:N films, meanwhile the co-doped ZnO films show higher crystallinity than the corresponding ZnO:Ga films.

Published in : Journal of Molecular Structure (2020), vol. 1206, 127773
DOI:10.1016/j.molstruc.2020.127773
Status : Postprint (Author's version)

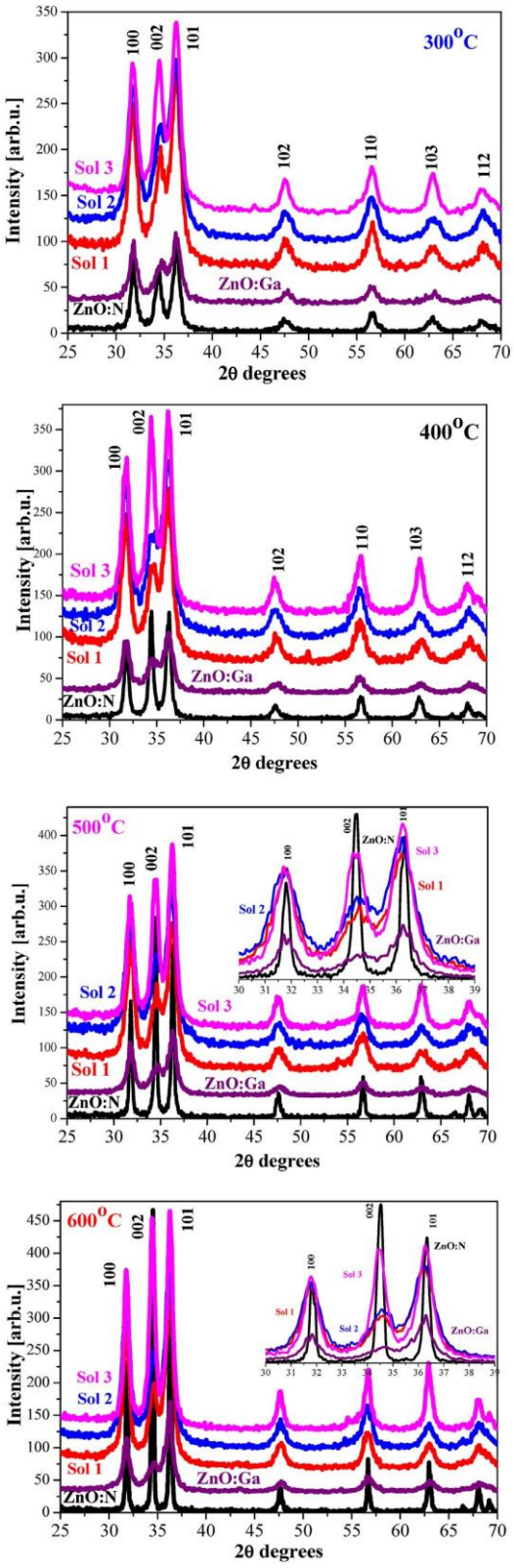

Fig. 1. XRD patterns of ZnO:N, ZnO:Ga and ZnO:N:Ga films, obtained from sol 1, sol 2 and sol 3. The films are annealed at the temperatures of 300–600 °C. The two insets present the enlarged images of XRD peaks 100, 002 and 100 of the annealed ZnO based films at 500 and 600 °C.

Published in : Journal of Molecular Structure (2020), vol. 1206, 127773
DOI:10.1016/j.molstruc.2020.127773
Status : Postprint (Author's version)

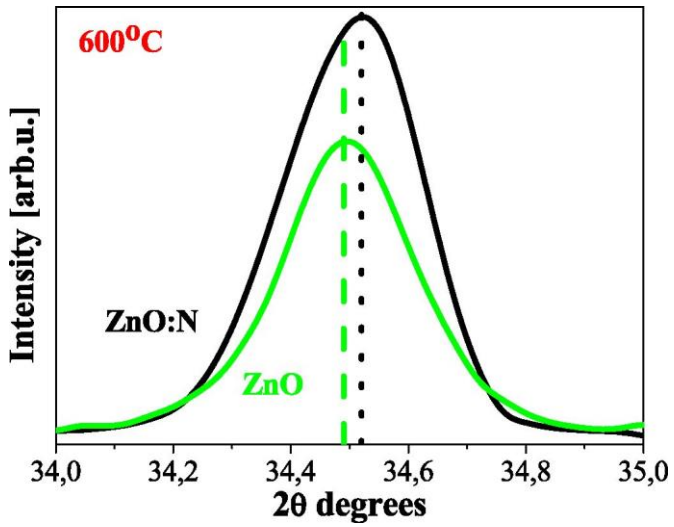

Fig. 2. XRD 002 peak of the sol-gel ZnO and ZnO:N films, annealed at 600 °C.

The average crystallite sizes are estimated by using the Scherrer equation on the (100), (002) and (101) difraction peaks. The obtained results are presented in **Fig. 3**. The crystallites of undoped ZnO and ZnO:N films grow greater with increasing the annealing temperatures. The greatest crystallite sizes are determined for the nitrogen doped ZnO films (for all thermal treatments). An increase in the crystallite sizes with nitrogen incorporation in ZnO structure is reported in literature [22,23]. On the other side, it is seen that Ga incorporation suppresses the crystallite growth. The crystallite sizes of Ga doped films are significantly smaller compared to those of undoped ZnO. A possible explanation is that there are changes of internal and external strain energy due to Ga impurities present in ZnO lattice matrix and oxygen defects [24] and/or Ga induces the increased number of nucleation centers [25] It has been previously reported that ZnO:Ga thin films manifest smaller grain size than undoped ZnO films [7,17].

(N, Ga) co-doped ZnO films also show considerable decrease of the crystallite sizes compared to those of ZnO and ZnO:N (see **Fig. 3a**). It can be seen that the obtained values of the co-doped samples despite the annealing temperatures are closed to that of ZnO:Ga films. The crystallite sizes of ZnO:N:Ga films, deposited from sol 3 (smallest Ga addition) are higher than those of ZnO:Ga films. Meanwhile, the co-doped ZnO films, derived from the sols 1 and 2 possess smaller crystallite sizes. It suggests that to the Ga presence and its concentration has a significant effect on the crystallite growth of (N, Ga) co-doped ZnO films. The annealing temperature influences considerably the crystallite sizes of ZnO and ZnO:N films. For the co-doped ZnO films, there is a slight tendency of increasing the crystallite sizes with raising the annealing temperatures.

Published in : Journal of Molecular Structure (2020), vol. 1206, 127773
DOI:10.1016/j.molstruc.2020.127773
Status : Postprint (Author's version)

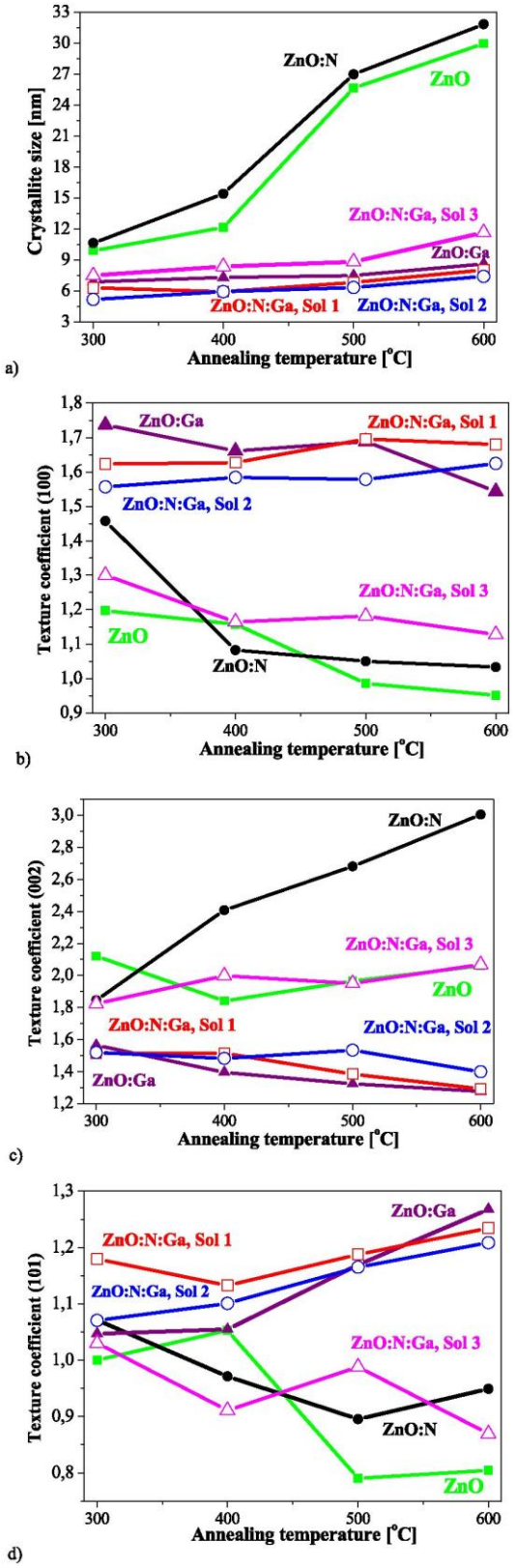

Fig. 3. The average crystallite sizes, determined from the (100), (002) and (101) difraction peaks for ZnO, ZnO:N, ZnO:Ga and co-doped ZnO films (a). The evolution of the texture coefficients for the (100), (002) and (101) difraction peaks with annealing temperatures are presented in **figures b**, **c** and **d**, respectively.

Published in : Journal of Molecular Structure (2020), vol. 1206, 127773
DOI:10.1016/j.molstruc.2020.127773
Status : Postprint (Author's version)

The signal intensities from the XRD planes contain information on preferential or random growth for polycrystalline thin films. The degrees of the preferential orientation of the three crystalline planes 100, 002 and 101 for undoped, N doped, Ga doped and (N, Ga) co-doped ZnO films have been estimated by calculating the corresponding texture coefficients (TC(hkl)). The texture coefficients (TC) are determined using the JCPDS card 01-070-8070, taking in mind the standard intensities for (100), (002), (101), (102), (110), (103), and (112) planes, respectively. A sample with randomly oriented crystallites yields TC(hkl) = 1 or lower, while the larger this value, the larger abundance of crystallites orientated at this (hkl) direction [26]. Furthermore, TC values between 0.00 and 1.00 indicate the lack of grains orientated in the certain direction. On the other hand, the larger of texture coefficient deviates from unity, the higher will be the preferred orientation of the film. The degree of the preferred orientation denoted by the XRD data calculations is presented in **Fig. 3b**, **c** and **d**.

It is seen that the highest TC values in (002) plane are observed for ZnO:N films for temperatures above 400 °C. It is obtained TC (002) = 3.0 for ZnO:N film, treated at 600 °C, which is a clear indication for texture and preferred growth. On the other hand, Ga doped ZnO films show the highest TC values for (100), suggesting that Ga atoms would suppress the (002) plane growth and the preferred orientation is changed to (100) plane. The ZnO:N:Ga films, deposited from sol 1 and 2 exhibit closer values for TC (100) and TC (002). ZnO:N:Ga (sol 3) films show higher values ofTC (002) comparing to ZnO:Ga and ZnO:N:Ga films, from sol 1 and 2. The estimated texture coefficients show that nitrogen concentration in the N, Ga co-doped ZnO films effects considerably the preferred orientation of the crystallites. The changes of preferred orientation due to the effect of N and Cu co-doping in ZnO lattice are also reported [27]. It can be concluded that the crystallization of ZnO:Ga and ZnO:N:Ga (sol 1 and 2) films is quite poor and the crystallites are more randomly oriented.

The lattice parameters *a* and *c* are estimated from the XRD data and the results are presented in **Fig. 4**. The changes in the lattice parameters are mainly caused by impurities, lattice defects, vacancies, deposition conditions and concentration of native imperfections in thin films. The *c* values of undoped ZnO are higher compared to Ga doped and N, Ga co-doped ZnO films, significantly lower c values are found for ZnO:Ga films. As Ga^{3+} holds a smaller ionic radius with respect to Zn^{2+}, thus substitution of Zn^{2+} with Ga^{3+} at lattice sites could decrease the lattice constant [28]. The lattice parameter c of the nitrogen doped ZnO films has interesting behaviour, a very strong dependence on the annealing temperatures is revealed. For 300 and 400 °C treated ZnO:N films, the c is increased, revealing the highest values among the studied sol-gel films. After annealing at 500 and 600 °C, the *c* lattice constan drops to the values lower than those of undoped ZnO, treated at these temperatures. The larger lattice constants can be attributed to the internal tensile stress due to N atom incorporation in the ZnO lattice [13]. After the annealing, the structural qualities of the ZnO:N films are enhanced and the defects states are possibly reduced. The ZnO:N:Ga films possess lower c values, most probably due to the gallium doping. The highest *c* parameter and much closer to thus of undoped films is observed for ZnO:N:Ga films, derived from

Published in : Journal of Molecular Structure (2020), vol. 1206, 127773
DOI:10.1016/j.molstruc.2020.127773
Status : Postprint (Author's version)

sol 3, where is the smallest Ga concentration. These results suggest that ZnO:N:Ga (sol 3) and undoped ZnO films have the lowest lattice stress, almost independent on the annealing temperatures.

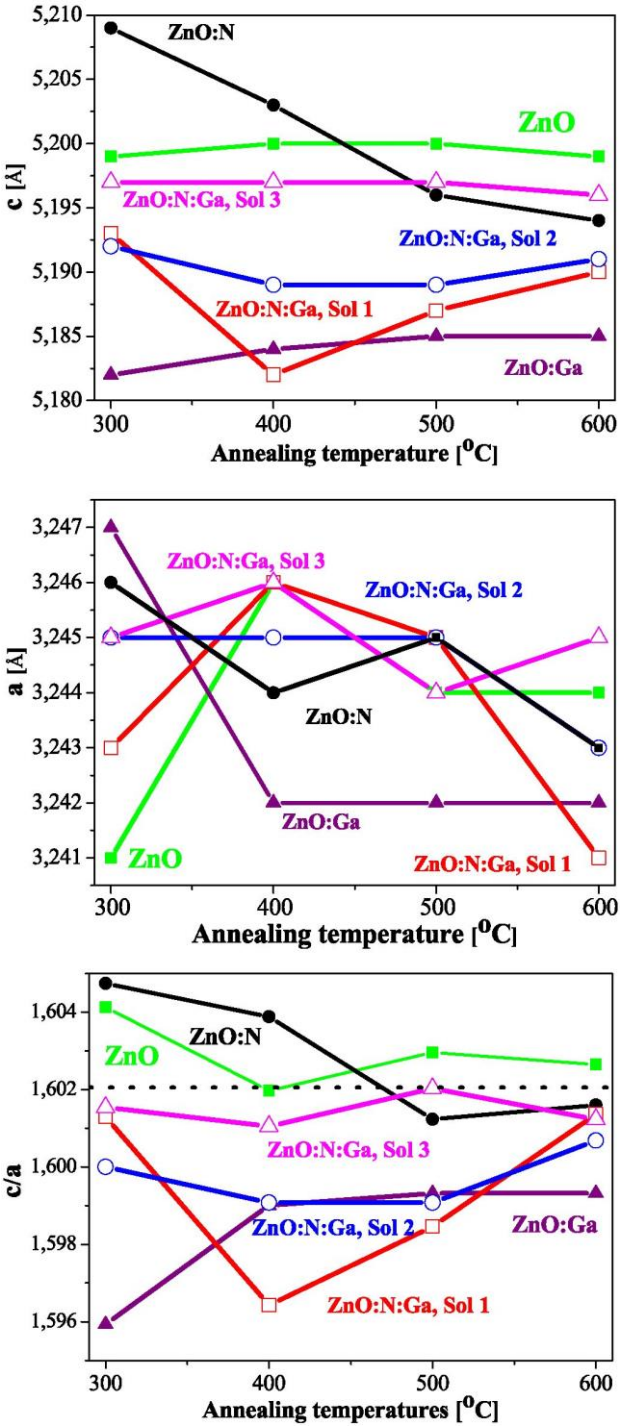

Fig. 4. Lattice parameters a, c and ratio c/a determined from XRD data for ZnO and doped ZnO films. The standard lattice parameters are a = 3,24,890 Å and c = 5,20,490 Å, c/a is 1,60,205 (according to the JCPDS card 01-070-8070).

Published in : Journal of Molecular Structure (2020), vol. 1206, 127773
DOI:10.1016/j.molstruc.2020.127773
Status : Postprint (Author's version)

It is also found that the c/a ratio values are almost constant for ZnO and ZnO:N:Ga films and their values are in a very good agreement with the standard value (1,60,205), which is close to the ideal value for hexagonal cell c/a = 1.633. It is well known that the crystal structure of ZnO deviates from the ideal wurtzite by the change in the ratio of the lattice parameters - c/a ratio. This observed constant of the c/a ratio proves once more that the hexagonal structure practically does not change upon co-doping with certain doping concentrations, on the other hand the single nitrogen and gallium incorporations and the ZnO:N:Ga films (sols 1, 2) result in some distortion of the wurtzite structure, more pronounced effect for the lower annealing temperatures. The deviations from the ideal value are due to the microstrains and the concentration of defects in the crystal lattice structure.

XRD analysis reveals that Ga concentration strongly influences on the crystallization behaviour, crystallite sizes and texture coefficients. From **Figs. 1** and **3**, it can be seen that decreasing the gallium component, the crystallization is enhanced and the biggest crystallite sizes among the co-doped ZnO samples are estimated for ZnO:N:Ga films, derived from sol 3. The same tendency is observed for TC values, where the Ga effect can be observed as for all texture coefficients of (100), (002) and (101) reflections. ZnO:Ga and ZnO:N:Ga films, obtained from sol 1 and 2 show similar values. On the other hand, the structural properties of the ZnO:N:Ga films (sol 3) is more considerable influenced by nitrogen doping.

FTIR spectroscopy is applied as a supplementary study to XRD analysis. The absorption bands (their shape, intensity, position) are influenced by crystalline structure, degree of crystallinity, chemical composition, particle sizes, forms and film morphology [29]. The effects of Ga and N additions as well as their co-doping on the structural bonding of ZnO films have been investigated by FTIR spectroscopy. The spectra are recorded for ZnO:N, ZnO:Ga and ZnO:N:Ga films, treated at different annealing temperatures (see **Fig. 5**), comparison with undoped ZnO films is also discussed. Detailed FTIR study of undoped ZnO and ZnO:Ga films is previous reported [19], where the gallium concentration varies and it is lower than the gallium doping used in this research.

Published in : Journal of Molecular Structure (2020), vol. 1206, 127773
DOI:10.1016/j.molstruc.2020.127773
Status : Postprint (Author's version)

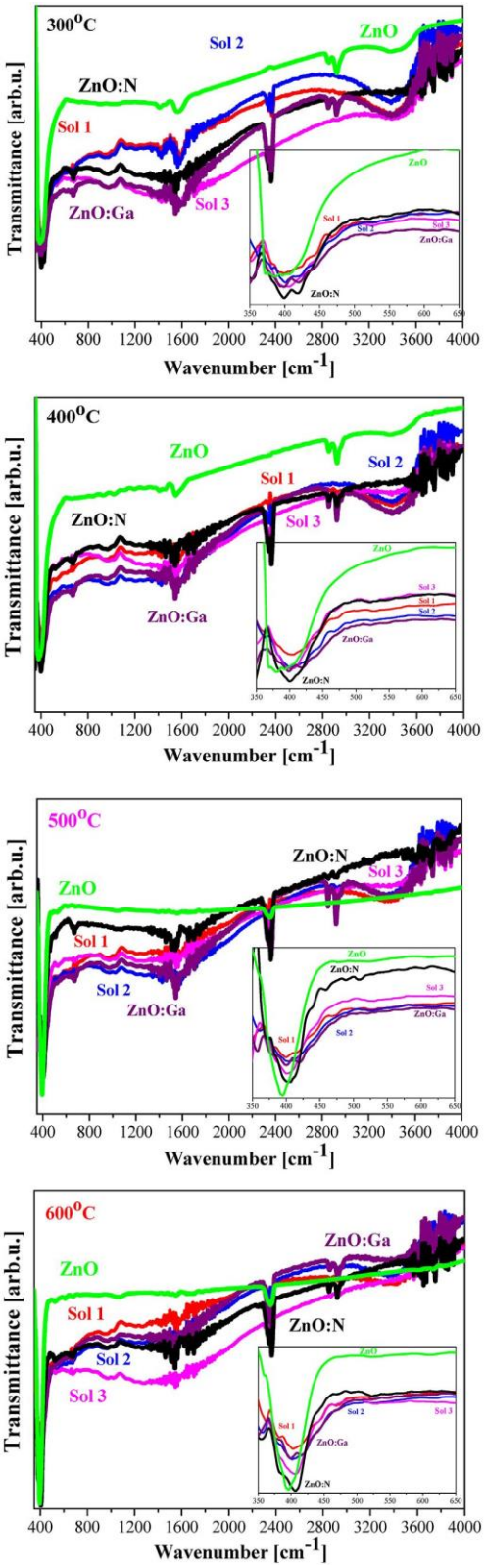

Fig. 5. FTIR spectra of the undoped ZnO, ZnO:N, ZnO:Ga and ZnO:N:Ga films, obtained from sol 1, sol 2 and sol 3. The studied films are annealed at different temperatures, ranging from 300 to 600 °C. The inset figures show the enlarged images of the wavenumber region from 350 to 650 cm^{-1}.

Published in : Journal of Molecular Structure (2020), vol. 1206, 127773
DOI:10.1016/j.molstruc.2020.127773
Status : Postprint (Author's version)

FTIR analysis reveals few absorption bands related to OH stretching vibrations in the spectral range 1000–4000 cm^{-1} [30]. These bands around 3400 cm^{-1} are well expresssed in the spectra of the films, treated at lower annealing temperatures and they vanish after high temperature treatments above 400 °C. It must be noted that for ZnO:N films, they are clearly manifested only for 300 °C treated samples and for the higher annealing temperatures, the bands are almost missing. Meanwhile, ZnO:Ga and ZnO:N:Ga films possess evident absorption features due to water inclusions even after annealing at the highest temperature – 600 °C. The undoped ZnO films show very weak bands associated with the stretching and bending vibrations of hydroxyl groups and they disappear after the annealings at temperature above 400 °C [19]. The IR lines at 2960 and 2850 cm^{-1} are assigned to C–H stretching modes [30]. The absorption features at 2340 cm^{-1} are due to atmospheric CO_2 [31]. The 1550 and 1440 cm^{-1} lines are associated with asymmetric and symmetric stretching vibrations of (COO^-) groups [32]. The IR band at 1020 cm^{-1} (appearing for all samples, especially after high temperature treatments) is related to the native oxide on the silicon substrate used [33].

The spectral part from 350 to 1000 cm^{-1} is the fingerprint region, where metal oxides generally exhibit characteristic absorption bands due to metal-oxygen vibrations. The characterestic IR absorption bands of gallium oxides are reported to be located: at 690 -621 cm^{-1} – Ga–O bonding [30]; at 457, 652 cm^{-1} related to Ga_2O bending mode [30] and at 680 cm^{-1} – Ga–O stretching vibrations [34]. The absorption bands of Ga–O bonding in GaO_6 octahedra can be found at 466, 478, 572 and 667 cm^{-1} and Ga–O bending and stretching vibrations of GaO_4 tetrahedra appear at 630, 656 and 730 cm^{-1} [35,36]. Other reported IR peaks are located at 613 and 459 cm^{-1} (assigned to Ga–O–Ga and Ga–O vibration of β-Ga_2O_3) and at 650 and 480 cm^{-1} (due to α-Ga_2O_3) [37]. It is known that some of the characteristic IR bands of ZnO are also appeared at these frequencies. The nitrogen incorporation in ZnO is reported to be manifested by a vibrational mode at 886 cm^{-1} (related to substitutional hydrogen at oxygen site bound to the lattice Zn site) [38]. The modification of the absorption bands of hydroxyl group vibrations can be associated with nitrogen doping and new broad bands at 3020 cm^{-1} or at 3146 cm^{-1} can be recognezised as N–H mode [39,40]. The observation of modifications of the C–H, O–H and N–H bonds can also be used an evidence for nitrogen doping [39].

ZnO:N films reveal strong and broad absorption features around 400 cm^{-1}, which vary in shape and position with a shifting from 397 cm^{-1} (300 °C) to 407 cm^{-1} (600 °C). These bands are assigned to Zn–O stretching vibrations [38]. The IR lines at 420 and 522 cm^{-1} are attributed to the stretching vibrations of Zn–O in ZnO wurtzite structure [41]. The band at 660-670 cm^{-1} is due to Zn–O bonding [38]. The broad band at 969 cm^{-1} can be related to the deformation bands of C=O [42]. ZnO:Ga films exhibit considerably broader and weaker main absorption bands compared to those of undoped ZnO and ZnO:N films. They are located around 400 cm^{-1} (for all temperature treatments) assigned to characteristic stretching Zn–O bonds [38]. The low intensities and the broadness of these absorption features can be an indication of the reduced crystallization and the nanocrystalline nature of the films [43], a conclusion supported by XRD analysis. The weak lines at 660-670 cm^{-1}

Published in : Journal of Molecular Structure (2020), vol. 1206, 127773
DOI:10.1016/j.molstruc.2020.127773
Status : Postprint (Author's version)

and a broad band at 969 cm^{-1} are also seen. The weak lines at 740 cm^{-1} can be related to Ga–O stretching vibrations [35]. The broadness and splitting, observed for the main absorption bands in ZnO:Ga films may have contribution of the Ga–O bonding.

FTIR spectra of ZnO:N:Ga films, obtained from sol 1 present a stronger and sharper main absorption bands with increasing of the annealing temperatures. This band is shifted from 397 (300 °C). to 403 cm^{-1} (600 °C). The highest thermal treatment provokes an appearance of some new peaks at 360, 380 and 440 cm^{-1}. Other IR lines at 470, 525 and 590 cm^{-1} are observed. ZnO:N:Ga films (sol 2) have their main absorption feature at 404 cm^{-1} with weaker lines at 420, 445, 465, 525, 616, 665 and 960 cm^{-1}. Similar features are detected for ZnO:N:Ga films (sol 3) films as their main absorption bands are the strongest. The observed IR lines are assigned to Zn–O vibrations [44,45], the influence of Ga incorporation is observed in the band shapes. It is interesting to mark the weak absorption band at 841 cm^{-1} appeared in the spectra of 600 °C annealed ZnO:N and ZnO:N:Ga films (derived from the sol 2 and sol 3) can be proprosed to be related to nitrogen doping effect [38].

FTIR analysis reveal that nitrogen doping affects the absorption features (ZnO:N films). Obvious changes occur in the infrared transmittance spectra with gallium incorporation (ZnO:Ga films). The co-doping with N and Ga exhibits more complex influence, but the bands positions and shapes are changed and new absorption bands appear. The IR main line of ZnO:N (300 °C), ZnO:Ga (all annealing temperatures) and ZnO:N:Ga (sol 1, sol 2 for 300 and 600 °C) films vary from a broad single band to the splitting in doublet or three-band superposition. This can be resulted from new bondings due to dopant or from different geometrical shapes of particles [46]. The other possible explanation of this band splitting is ascribed to the variation of the oxygen defect density [47]. The higher the splitting degree, the higher is the oxygen defect density.

The transmittance and reflectance spectra of the sol-gel ZnO, ZnO:Ga and ZnO:N:Ga films have been measured in the spectral range of 240–1800 nm and their dependence on the thermal treatments is given in **Fig. 6**. As it has been reported previously [19,20], the transmittance of undoped ZnO films reveals a decrease after high temperature treatments. The change of the film transparency can be related to the light scattering induced by the greater crystallites and the crystallite boundaries of the annealed ZnO structures. The spesific excitonic absorption of the undoped ZnO films is found around 340 nm [48]. These features are better expressed after 500 and 600 °C annealing. These features are due to the excitonic absorption of ZnO. The excitonic peak of bulk ZnO is located near 373 nm. The excitonic peaks disappear in the transmittance spectra of ZnO:Ga and ZnO:N:Ga films. Excitonic peaks are not seen in the transmittance spectra of ZnO:Ga and ZnO:N:Ga films which may be related to the poor crystallinity of these films.

The gallium doping leads to an improvement of film optical quality [7,19]. The thermal procedures affect very slightly the transmittance and reflectance of the sol-gel derived ZnO:Ga films, the transmittance is 88–90% and the reflectance is 10–13% for the spectral range of 450–800 nm.

Published in : Journal of Molecular Structure (2020), vol. 1206, 127773
DOI:10.1016/j.molstruc.2020.127773
Status : Postprint (Author's version)

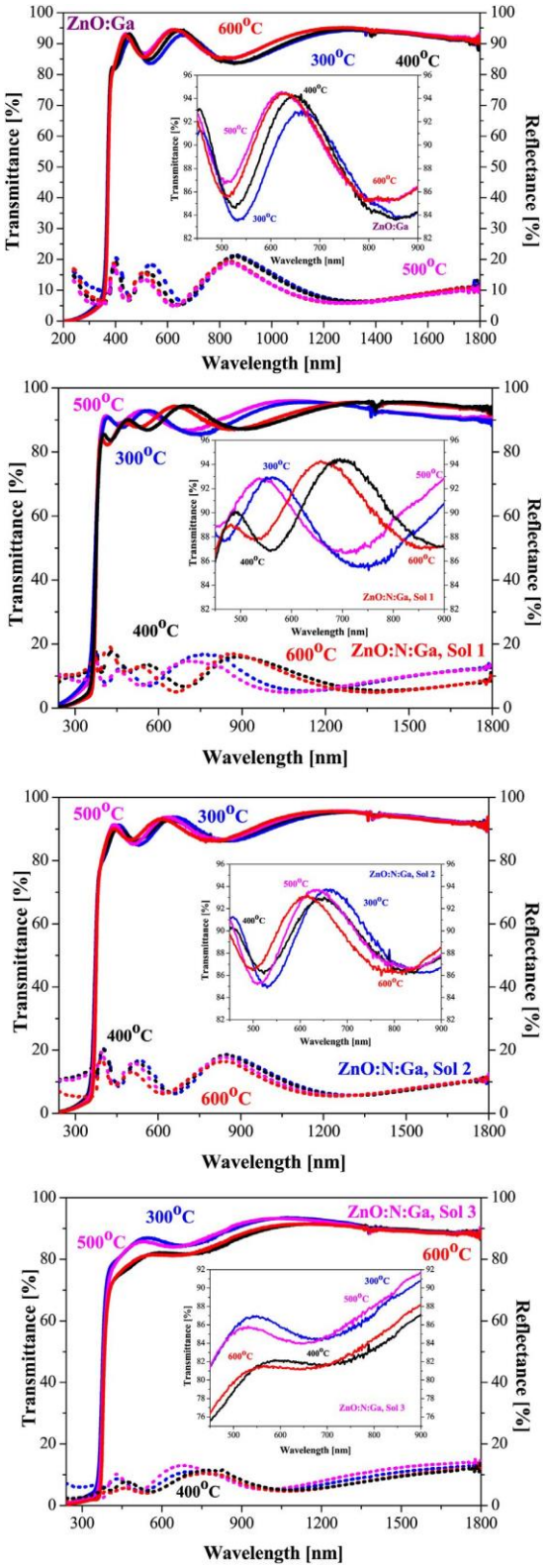

Fig. 6. Transmittance and reflectance spectra of ZnO:Ga and ZnO:N:Ga thin films, obtained from sol 1, sol 2 and sol 3. The studied films are thermally treated at different temperatures, ranging from 300 to 600 °C. The solid lines represent transmittance and the dotted lines – reflectance, respectively. The inset figures show the transmittance in the spectral range 450–900 nm in dependence of the annealling temperatures.

Published in : Journal of Molecular Structure (2020), vol. 1206, 127773
DOI:10.1016/j.molstruc.2020.127773
Status : Postprint (Author's version)

The annealing temperatures do not modify significantly the transmittance and reflectance spectra of the N and Ga co-doped ZnO films as it is shown in **Fig. 6**. For all thermal treatments, it can be observed that the ZnO:Ga and ZnO:N:Ga films, obtained from sol 1 and 2 possess the best transparency with average transmittance above 88%. ZnO:N:Ga sol 3 films exhibit a slightly lower transmittance (average transmittance 82–86.4%, depending on the annealing), but still their film transparency is enhanced comparing to undoped ZnO films (average transmittance 78–83%, depending on the annealing). This can be assigned to the smoother surfaces of co-doped ZnO compared to the rougher ZnO morphology (SEM micrographs presented below) and XRD analysis reveals greater crystallites for undoped ZnO films, respectively higher light scattering. The crystallites sizes of ZnO:Ga and ZnO:N:Ga films are considerably smaller. **Fig. 7** presents the comparison of the transmittance and reflectance spectra of sol-gel undoped ZnO, ZnO:Ga and ZnO:N:Ga films, treated at 600 °C. It must be pointed out that undoped ZnO films change the transmittance with thermal treatments and their transparency is worsening with increasing the annealing temperatures. The doped and co-doped ZnO films have no such optical behaviour. On the other hand, the reflectance of ZnO films is increased with annealing. The reflectances of ZnO:N:Ga films, obtained from sol 3 have the lowest values from 7.6 to 9.3%, while the other co-doped ZnO films shows average reflectance in the range of 11–13% for the spectral range 450–900 nm.

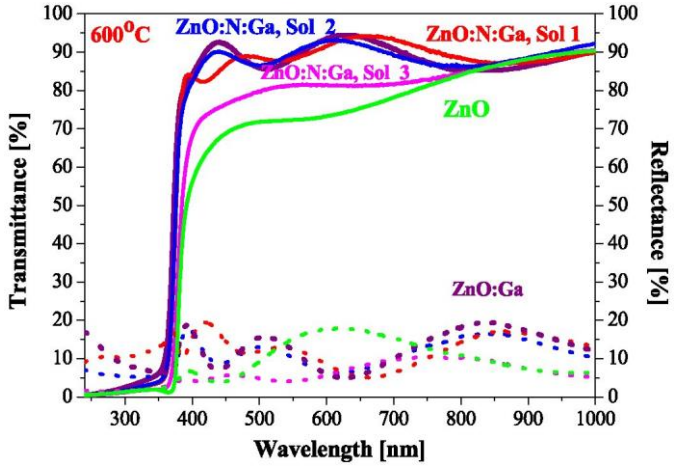

Fig. 7. Comparison of the transmittance and reflectance spectra of ZnO, ZnO:Ga and ZnO:N:Ga films, annealed at 600 °C for the spectral range 240–1000 nm.

Fig. 7 clearly indicates that Ga doping induces the improved transparency as ZnO:Ga and ZnO:N:Ga (sol 1, sol 2) films reveal the highest transmittance in the visible spectral range. The lowest Ga content results in lower transparency of ZnO:N:Ga (sol 3) films, but still better than compared to pure ZnO films.

Published in : Journal of Molecular Structure (2020), vol. 1206, 127773
DOI:10.1016/j.molstruc.2020.127773
Status : Postprint (Author's version)

The optical band gaps, E_g, of the sol-gel films are estimated from the transmittance spectrophotometric data and the results are presented in **Fig. 8**. A number of factors can influence on optical band gap, including grain sizes, lattice parameters and bond lengths, film crystallinity and crystal imperfections presence of impurities and/or other defects, lattice strain and stress [49,50]. Itis known that gallium introduction could enhance the optical band gap and such band gap widening is reported in literature and it is explained with the Burstein –Moss effect (i.e. shift of the Fermi level caused by an increased conduction electron concentration) [7,51]. The nitrogen doping in ZnO is found to reduce the optical band gap, probably due to the existence of Zn–N bonds having smaller ionocity of Zn–O bonds [52,53].

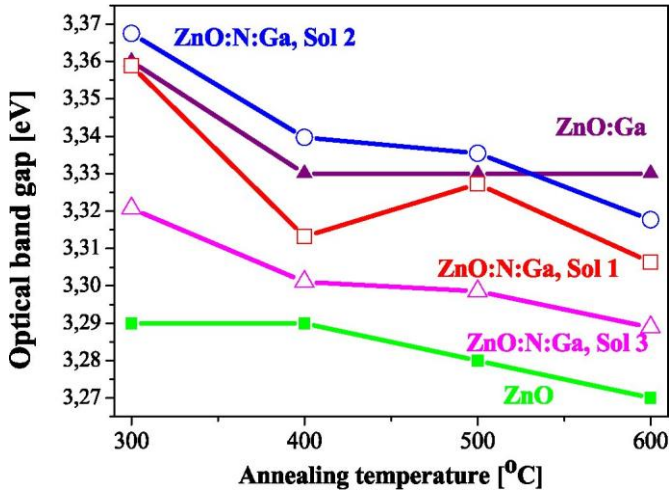

Fig. 8. Dependence of the optical band gap values of ZnO, ZnO:Ga and ZnO:N:Ga films on the annealing temperatures.

The optical band gap values of ZnO:Ga and ZnO:N:Ga films are higher than those of undoped ZnO films. XRD study shows that the crystallite sizes of the ZnO based films diminished with gallium doping thus the quantum size can play an important role in the increasing of the band-gaps [54]. The lattice stress can also contribute to the larger band gaps of co-doped ZnO films as it is known that when the stress is tensile in nature, it exibits blue shift of E_g (optical band gap increases) and respectively the compressive stress results in red shift of E_g Ref. [55]. The results of the optical band gap reveal that ZnO and ZnO:N:Ga films (sol 3) have closer values, remaining the similar tendency of the tensile stress change (closed values of lattice parameter *c*) although their crystalite sizes are very different. The co-doped ZnO films possess optical band gaps influence by Burstein –Moss effect, crystallite sizes and lattice stress. The calculated values of E_g for ZnO, ZnO:Ga and ZnO:N:Ga films are in the range of the reported data for ZnO based nanostructures [24,56].

The morphological microstructure study of ZnO and ZnO:N:Ga films, annealed at 600 °C is performed by FESEM technique. The film morphology has been analysed using different magnifications. SEM micrographs of the sol-gel undoped ZnO film (see **Fig. 9**), reveal an interesting surface with irregular fibre-like and wrinkle network structure (magnification 10X and spatial resolution of 3 μm). The width of the wrinkes (**Fig. 9a**) is 270–440 nm. In closer observation (**Fig.**

Published in : Journal of Molecular Structure (2020), vol. 1206, 127773
DOI:10.1016/j.molstruc.2020.127773
Status : Postprint (Author's version)

9b), ZnO surface looks porous with irregullar grains in shapes and forms. The grain sizes vary roughly from 30 to 100 nm. Similar wrinkled network morphology has been reported by other researchers for sol-gel spin-coated ZnO films [57,58].

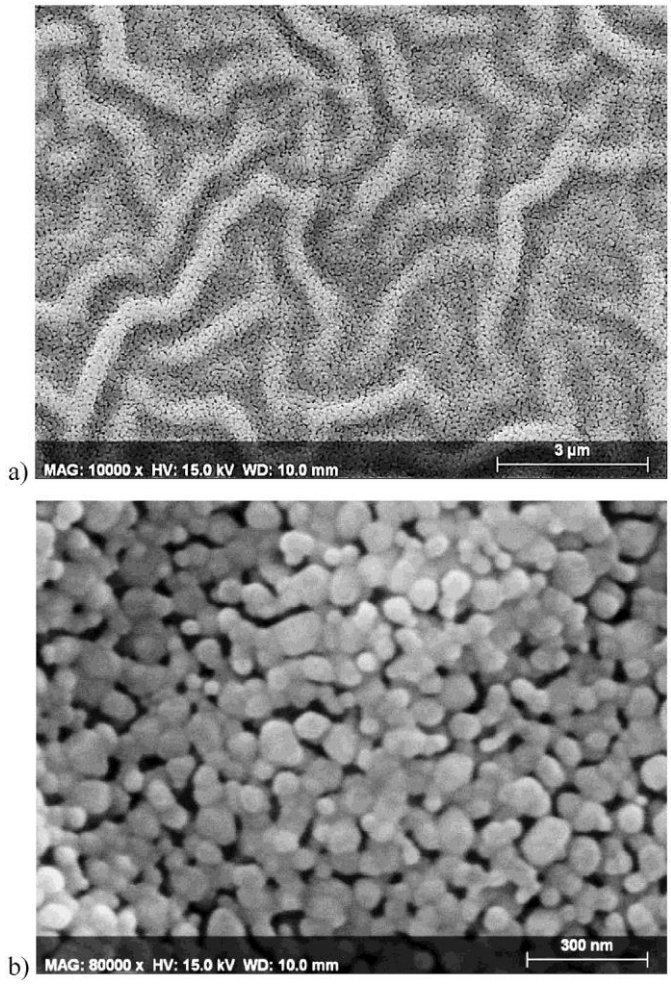

Fig. 9. Plane view SEM migrographs with different magnifications of undoped ZnO film, thermally treated at 600 °C.

Fig. 10 presents SEM micrographs of ZnO:N:Ga films, obtained from the three sols and annealed at 600 °C. It can be clearly observed that the gallium and nitrogen co-doping considerably modifies the film morphology. The film morphologies of ZnO:N:Ga films, obtained from sol 1 and sol 2 possess closed packed grained structures with no wrinkles or fibers despite the resolutions used (magnification 10X and spatial resolution of 3 µm). Meanwhile, a wrinkle-like microstructure has been found for ZnO:N:Ga film, derived from sol 3. The observed film morphology is quite differing from that of the undoped ZnO, presented in **Fig. 9**. The wrinkles, in the case of ZnO:N:Ga film, deposited from sol 3 are much thinner with greater density than the corresponding wrinkled network of ZnO film. The micrograph at the higher magnification of ZnO:N:Ga (sol 3) exhibits grained morphology with very fine grains and randomly distributed bigger particles. The size of the smaller grains are in the range of 10–23 nm (with different shapes and sizes) and the greater

Published in : Journal of Molecular Structure (2020), vol. 1206, 127773
DOI:10.1016/j.molstruc.2020.127773
Status : Postprint (Author's version)

particles are at the rate up to 70 nm. The film morphologies of ZnO:N:Ga (sol 1) and ZnO:N:Ga (sol 2) look very similar – grained structures, close packed with no clear grain boundaries. The particles sizes vary from 11 to 32 nm (for ZnO:N:Ga film, obtained from sol 1) and 8–11 nm (for ZnO:N:Ga (sol 2)), but it must be noted that the grains size is diffucult to determine as the sharpness of the grain boundaries diminishes.

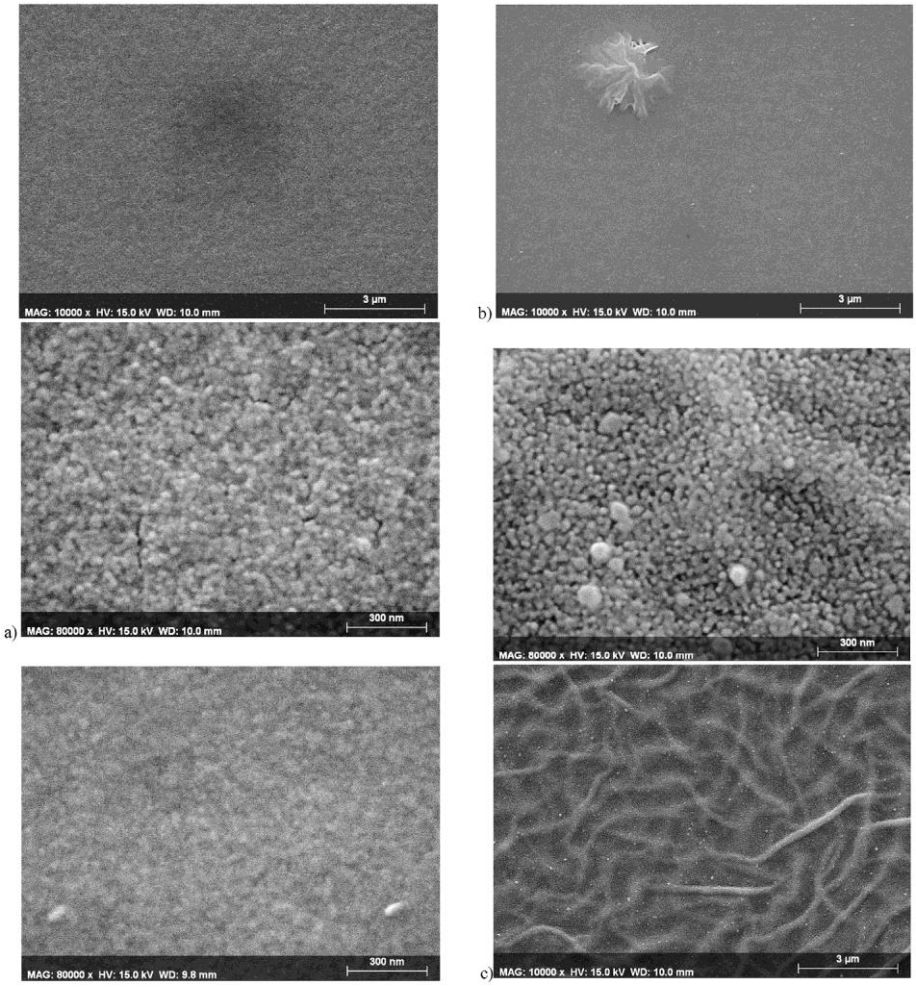

Fig. 10. Plane view SEM migrographs with different magnifications of a) ZnO:N:Ga 1, b) ZnO:N:Ga 2 and c) ZnO:N:Ga 3 films, thermally treated at 600 °C. The artifact seen in the higher magnification image of ZnO:N:Ga 2 film should be ignored.

It is found out that the grain and crystalite sizes are different, determined from FESEM and XRD studies. It is well known that the crystallite size is suggested to be the size of a coherently diffracting domain and is not necessarily to be the same as the particle size. On the other side, the XRD peak can be widened by defects and internal stress, and respectively the crystallite size calculated by Scherrer equation is smaller than the actual value [59]. For all studied films, the grain sizes are greater than the values from XRD estimation (**Fig. 3**), nevertheless the tendency is remained.

Published in : Journal of Molecular Structure (2020), vol. 1206, 127773
DOI:10.1016/j.molstruc.2020.127773
Status : Postprint (Author's version)

The wrinkle network is seemed to be dependent on both Ga and N doping, as it appears for ZnO:N:Ga film, obtained from sol 3. Previous SEM investigation [19] manifests that the wrinkle microstructure for the undoped ZnO film disappears with the galluim doping. The wrinkle formation of the sol-gel films has been induced by several possible reasons: 1) the increase in volumetric stress in the films and evaporation of the solvent [60], 2) lack of hydroxyl (or alkoxy) groups in the sols [60] or 3) release of mechanical stresses developed during densification and heat treatment of the films [61,62]. FTIR analysis exhibit very weak and broad absorption bands for the undoped ZnO films due to the stretching vibrations of hydroxyl groups (at 3300–3500 cm^{-1}) after 300 °C annealing, which vanished completely at the higher annealing temperatures [19,20]. In contrast to ZnO:Ga and ZnO:N:Ga films, where the absorption lines due to hydroxyl groups are detected even after the highest annealing (600 °C, **Fig. 5**).

The surface micrographs clearly manifest that the two dopants change the film structure and morphology, the wrinkle network is surpressed, closed packed grained structures are developed. The ZnO:N:Ga film morphologies are smoother than the undoped ZnO surface, which can explained their improved film transparency. The transmittance of ZnO:N:Ga (sol 3) film, annealed at 600 °C (**Fig. 7**) is worsened compared to the other ZnO:N:Ga films, derived from sol 1 and 2 and this can be related to the rougher wrinkle network.

4. Conclusions

The sol-gel technology has been successfully applied for depositing ZnO:N, ZnO:Ga and co-doped ZnO:N:Ga thin films. ZnO based films are obtained by the spin coating on Si and quartz subtrates. The structural, morphological and optical properties of the sol-gel ZnO:N:Ga thin films with different nitrogen and gallium concentrations are characterized. XRD studies of the single doped and (N, Ga) co-doped ZnO films reveal that the films crystallize in the hexagonal wurtzite crystal phase with no impurity fractions. The ZnO:N films manifest improved crystalization wth stronger and sharper XRD lines compared to undoped ZnO. The gallium incorporation in ZnO deteriorates the film crystallinity. The crystallization of ZnO:N:Ga films diminishes comparing to undoped ZnO and ZnO:N films. Crystallite sizes, texture coefficients and lattice parameters for all studied films have been determinined and compared. The obtained results proposes that ZnO:N:Ga 3 and undoped ZnO films have the lowest tensile lattice stress values almost independent on the annealing temperatures. (N, Ga) codoped ZnO films show a considerable decrease of the crystallite sizes compared to those of undoped ZnO and ZnO:N. FTIR study shows that Ga and N affects the absorption bands shapes and positions. ZnO:Ga and ZnO:N:Ga films exhibit high transparency across the visible spectral range and their transmittance is improved compared to undoped ZnO films. It has been found that the optical band gap of ZnO:Ga and ZnO:N:Ga films are enlarged than those of undoped ZnO. The FESEM micrographs clearly manifest that nitrogen and gallium co-doping significally modifies the film morphology, the wrinkle network of undoped ZnO films is surpressed and closed packed grained structures are observed. The ZnO:N:Ga film surfaces look more uniform and smoother compared to ZnO. The film morphology features can explain the

Published in : Journal of Molecular Structure (2020), vol. 1206, 127773
DOI:10.1016/j.molstruc.2020.127773
Status : Postprint (Author's version)

transmittance difference of ZnO and ZnO:N:Ga films, obtained from the synthesized sols with different nitrogen and gallium concentrations.

CRediT authorship contribution statement

T. Ivanova: Conceptualization, Methodology, Writing - original draft, Writing - review & editing, Investigation. **A. Harizanova**: Investigation, Visualization, Writing - original draft, Conceptualization, Validation. **T. Koutzarova**: Investigation, Validation. **B. Vertruyen**: Investigation, Validation. **R. Closset**: Investigation, Visualization.

References

[1] A. Wei, L. Pan, W. Huang, Recent progress in the ZnO nanostructure-based sensors, Mater. Sci. Eng. B Solid-State Mater. Adv. Technol. 176 (2011) 1409–1421.

[2] S. Chu, M. Olmedo, Z. Yang, J. Kong, J. Liu, Electrically pumped ultraviolet ZnO diode lasers on Si, Appl. Phys. Lett. 93 (18) (2008) 181106.

[3] J. Wang, R. Chen, L. Xiang, S. Komarneni, Synthesis, properties and applications of ZnO nanomaterials with oxygen vacancies: a review, Ceram. Int. 44 (7) (2018) 7357–7377.

[4] C. Lung, M. Toma, M. Pop, D. Marconi, A. Pop, Characterization of the structural and optical properties of ZnO thin films doped with Ga, Al and (Al+Ga), J. Alloys Compd. 725 (2017) 1238–1243.

[5] M. Samadi, M. Zirak, A. Naseri, E. Khorashadizade, A.Z. Moshfegh, Recent progress on doped ZnO nanostructures for visible-light photocatalysis, Thin Solid Films 605 (2016) 2–19.

[6] A. Kalaivanan, S. Perumal, N. Pillai, K. Sivaramamoorthy, K.R. Muralie, Characteristics of gallium doped ZnO thin films deposited by sol gel dip coating, ECS Trans. 19 (27) (2009) 65–70.

[7] S. Chen, G. Carraro, D. Barreca, A. Sapelkin, W. Chen, X. Huang, Q. Cheng, F. Zhang, R. Binions, Aerosol assisted chemical vapour deposition of Ga-doped ZnO films for energy efficient glazing: effects of doping concentration on the film growth behaviour and opto-electronic properties, J. Mater. Chem. 3 (2015) 13039–13049.

[8] J. Xu, R. Ott, A.S. Sabau, Z. Pan, F. Xiu, J. Liu, J.-M. Erie, D.P. Norton, Generation of nitrogen acceptors in ZnO using pulse thermal processing, Appl. Phys. Lett. 92 (2008) 151112.

[9] A. Valour, F. Cheviré, F. Tessier, F. Grasset, B. Dierre, T. Jiang, E. Faulques, C. Laurent, S. Jobic, Preparation of nitrogen doped zinc oxide nanoparticles and thin films by colloidal route and low temperature nitridation process, Solid State Sci. 54 (2016) 30–36.

[10] V. Tiron, I. Velicu, D. Stanescu, H. Magnan, L. Sirghi, High visible light photocatalytic activity of nitrogen-doped ZnO thin films deposited by HiPIMS, Surf. Coating. Technol. 324 (2017) 594–600.

[11] Z.Y. Xiao, Y.C. Liu, R. Mu, D.X. Zhao, J.Y. Zhang, Stability of p-type conductivity in nitrogen-doped ZnO thin film, Appl. Phys. Lett. 92 (2008), 052106.

Published in : Journal of Molecular Structure (2020), vol. 1206, 127773
DOI:10.1016/j.molstruc.2020.127773
Status : Postprint (Author's version)

[12] Ü. Özgür, Ya I. Alivov, C. Liu, A. Teke, M.A. Reshchikov, S. Doğan, V. Avrutin, S.-J. Cho, H. Morkoç, A comprehensive review of ZnO materials and devices, J. Appl. Phys. 98 (2005), 041301.

[13] S. Dhara, P.K. Giri, Stable p-type conductivity and enhanced photoconductivity from nitrogen-doped annealed ZnO thin film, Thin Solid Films 520 (2012) 5000–5006.

[14] W.S. Noh, Y.A. Lee, Y.H. Lee, Y.W. Heo, J.J. Kim, Effect of oxygen pressure on the p-type conductivity of Ga, P co-doped ZnO thin film grown by pulsed laser deposition, Ceram. Int. 42 (2016) 4136–4142.

[15] T. Yamamoto, Codoping for the fabrication of p-type ZnO, Thin Solid Films 420–421 (2002) 100–106.

[16] F.W. Xie, P. Yang, P. Li, L.Q. Zhang, First-principle study of optical properties of (N, Ga) codoped ZnO, Optic Commun. 285 (2012) 2660–2664.

[17] L.C.K. Liau, J.S. Huang, Effect of indium- and gallium-doped ZnO fabricated through sol-gel processing on energy level variations, Mater. Res. Bull. 97 (2018) 6–12.

[18] N.R.S. Farley, C.R. Staddon, L. Zhao, K.W. Edmonds, B.L. Gallagher, D.H. Gregory, Sol-gel formation of ordered nanostructured doped ZnO films, J. Mater. Chem. 14 (2004) 1087–1092.

[19] T. Ivanova, A. Harizanova, T. Koutzarova, B. Vertruyen, B. Stefanov, Structural and morphological characterization of sol-gel ZnO: Ga films: effect of annealing temperatures, Thin Solid Films 646 (2018) 132–142.

[20] T. Ivanova, A. Harizanova, T. Koutzarova, B. Vertruyen, Facile deposition of ZnO:Cu films: structural and optical characterization, Mater. Sci. Semicond. Process. 30 (2015) 561–570.

[21] S.Y. Tsai, Y.M. Lu, M.H. Hon, Fabrication of low resistivity p-type ZnO thin films by implanting N^+ ions, J. Phys. Conf. 100 (2008), 042037.

[22] I. Mouritys, P. Silva, G. Byzynski, C. Ribeiro, E. Longo, Different dye degradation mechanisms for ZnO and ZnO doped with N (ZnO:N), J. Mol. Catal. Chem. 417 (2016) 89–100.

[23] J.A. Oliveira, A.E. Nogueira, M.C.P. Gonçalves, E.C. Paris, C. Ribeiro, G.Y. Poirier, T.R. Giraldi, Photoactivity of N-doped ZnO nanoparticles in oxidative and reductive reactions, Appl. Surf. Sci. 433 (2018) 879–886.

[24] C. Lung, M. Toma, M. Pop, D. Marconi, A. Pop, Characterization of the structural and optical properties of ZnO thin films doped with Ga, Al and (Al+Ga), J. Alloys Compd. 725 (2017) 1238–1243.

[25] M. Yilmaz, Investigation of characteristics of ZnO:Ga nanocrystalline thin films with varying dopant content, Mater. Sci. Semicond. Process. 40 (2015) 99–106.

[26] S. Sönmezoglu, E. Akma, Improvement of physical properties of ZnO thin films by tellurium doping, Appl. Surf. Sci. 318 (2014) 319–323.

[27] M.N.H. Liton, M.K.R. Khan, M.M. Rahman, M.M. Islam, Effect of N and Cu doping on structure, surface morphology and photoluminescence properties of ZnO thin films, J. Sci. Res. 7 (1–2) (2015) 23–32.

[28] S. Liang, X. Bi, Structure, conductivity, and transparency of Ga-doped ZnO thin films arising from thickness contributions, J. Appl. Phys. 104 (2008) 113533.

[29] Z. Petrovic, M. Ristic, S. Music, Development of ZnO microstructures produced by rapid hydrolysis of zinc acetylacetonate, Ceram. Int. 40 (7) (2014) 10953–10959.

Published in : Journal of Molecular Structure (2020), vol. 1206, 127773
DOI:10.1016/j.molstruc.2020.127773
Status : Postprint (Author's version)

[30] J. Yang, Y. Zhao, R.L. Frost, Infrared and infrared emission spectroscopy of gallium oxide α-GaO(OH) nanostructures, Spectrochim. Acta A 74 (2) (2009) 398–403.

[31] L.S. Rao, T.V. Rao, Sd Naheed, P.V. Rao, Structural and optical properties of zinc magnesium oxide nanoparticles synthesized by chemical co-precipitation, Mater. Chem. Phys. 203 (2018) 133–140.

[32] G. Srinet, R. Kumar, V. Sajal, Optical and magnetic properties of Mn doped ZnO samples prepared by solid state route, J. Mater. Sci. Mater. Electron. 25 (7) (2014) 3052–3056.

[33] T. Gougousi, Z. Chen, Deposition of yttrium oxide thin films in supercritical carbon dioxide, Thin Solid Films 516 (2008) 6197–6204.

[34] G. Sinha, D. Ganguli, S. Chaudhuri, Ga_2O_3 and GaN nanocrystalline film: reverse micelle assisted solvothermal synthesis and characterization, J. Colloid Interface Sci. 319 (2008) 123–129.

[35] A. Dulda, Morphology controlled synthesis of α-GaO(OH) nanoparticles: thermal conversion to Ga_2O_3 and photocatalytic properties, Adv. Mater. Sci. Eng. 2016 (2016) article ID 3905625.

[36] K. Girija, S. Thirumalairajan, G.S. Avadhani, D. Mangalaraj, N. Ponpandian, C. Viswanathan, Synthesis, morphology, optical and photocatalytic performance of nanostructured β-Ga_2O_3, Mater. Res. Bull. 48 (2013) 2296–2303.

[37] I. Winer, G.E. Shter, M. Mann-Lahav, G.S. Grader, Effect of solvents and stabilizers on sol-gel deposition of Ga-doped zinc oxide TCO films, J. Mater. Res. 26 (10) (2011) 1309–1315.

[38] R. Kumari, A. Sahai, N. Goswami, Effect of nitrogen doping on structural and optical properties of ZnO nanoparticles, Prog. Nat. Sci.: Met. Mater. Int. 25 (2015) 300–309.

[39] B.M. Keyes, L.M. Gedvilas, X. Li, T.J. Coutts, Infrared spectroscopy of polycrystalline ZnO and ZnO:N thin films, J. Cryst. Growth 287 (2005) 297–302.

[40] S.A. Al Rifai, B.A. Kulnitskiy, Synthesis and characterization of N-doped zinc oxide nanotetrapods, Russ. J. Phys. Chem. 90 (2016) 1049–1056.

[41] M. Zerdali, S. Hanizaoui, F.H. Teheran, P. Rogers, Growth of ZnO thin film on SiO2/Si substrate by pulsed laser deposition and study of their physical properties, Matt. Lett. 60 (2006) 504–508.

[42] M.A.R. Bonifácio, H.L. Lira, L.S. Neiva, R.H.G.A. Kiminami, L. Gama, Nanoparticles of ZnO doped with Mn: structural and morphological characteristics, Mater. Res. 20 (4) (2017) 1044–1049.

[43] M. El-Kemary, N. Nagy, I. El-Mehasseb, Nickel oxide nanoparticles: synthesis and spectral studies of interactions with glucose, Mater. Sci. Semicond. Process. 16 (2013) 1747–1752.

[44] R. Elilarassi, G. Chandrasekaran, Structural, optical and magnetic properties of nanoparticles of ZnO:Ni—DMS prepared by sol–gel method, Mater. Chem. Phys. 123 (2010) 450–455.

[45] N. Goswani, A. Sahni, Structural transformation in nickel doped zinc oxide nanostructures, Mater. Res. Bull. 48 (2013) 346–351.

[46] M. Ristić, M. Marciuš, Ž. Petrović, M. Ivanda, S. Musić, The influence of experimental conditions on the formation of ZnO fibers by electrospinning, Croat. Chem. Acta 87 (4) (2014) 315–320.

[47] H. Sudrajat, S. Babel, A novel visible light active N-doped ZnO for photocatalytic degradation of dyes, J. Water Process Eng. 16 (2017) 309–318.

[48] X.D. Li, T.P. Chen, P. Liu, Y. Liu, K.C. Leong, Effects of free electrons and quantum confinement in ultrathin ZnO films: a comparison between undoped and Al-doped ZnO, Optic Express 21 (12) (2013), 14131–13318.

[49] M.M. Hassan, W. Khan, A. Azam, A.H. Naqvi, Influence of Cr incorporation on structural, dielectric and optical properties of ZnO nanoparticles, J. Ind. Eng. Chem. 21 (2015) 283–291.

[50] H. Mahdhi, Z.B. Ayadi, S. Alaya, J.L. Gauffier, K. Djessas, The effects of dopant concentration and deposition temperature on the structural, optical and electrical properties of Ga-doped ZnO thin films, Superlattice. Microst. 72 (2014) 60–71.

[51] J.L. Zhao, X.W. Sun, H. Ryu, Y.B. Moon, Thermally stable transparent conducting and highly infrared reflective Ga-doped ZnO thin films by metal organic chemical vapor deposition, Opt. Mater. 33 (2011) 768–772.

[52] E.S. Tuzemen, K. Kara, S. Elagoz, D.K. Takci, I. Altuntas, R. Ezen, Structural and electrical properties of nitrogen-doped ZnO thin films, Appl. Surf. Sci. 318 (2014) 157–163.

[53] M. Hirai, A. Kumar, Effect of nitrogen doping on bonding state of ZnO thin films, J. Vac. Sci. Technol., A 25 (2007) 1534–1538.

[54] A. Khorsand Zak, W.A. Majid, M. Abrishami, R. Yousefi, X-ray analysis of ZnO nanoparticles by Williamson–Hall and size–strain plot methods, Solid State Sci. 13 (2011) 251–256.

[55] R. Ghosh, D. Basak, S. Fujihara, Effect of substrate-induced strain on the structural, electrical, and optical properties of polycrystalline ZnO thin films, J. Appl. Phys. 96 (2004) 2689–2692.

[56] J. Ungula, B.F. Dejene, H.C. Swart, Band gap engineering, enhanced morphology and photoluminescence of un-doped, Ga and/or Al-doped ZnO nanoparticles by reflux precipitation method, J. Lumin. 195 (2018) 54–60.

[57] M. Yilmaz, Z. Caldiran, A.R. Deniz, S. Aydogan, R. Gunturkun, A. Turut, Preparation and characterization of sol–gel-derived n-ZnO thin film for Schottky diode application, Appl. Phys. A 119 (2015) 547–552.

[58] M. Wang, W. Liang, Y. Yang, J. Yang, X. Cheng, S.H. Hahn, E.J. Kim, Sol-gel derived transparent conducting ZnO:Al thin films: effect of crystallite orientation on conductivity and self-assembled network texture, Mater. Chem. Phys. 134 (2012) 845–850.

[59] A.A. Othman, M.A. Ali, E.M.M. Ibrahim, M.A. Osman, Influence of Cu doping on structural, morphological, photoluminescence, and electrical properties of ZnO nanostructures synthesized by ice-bath assisted sonochemical method, J. Alloys Compd. 683 (2016) 399–411.

[60] S.J. Kwon, J.H. Park, J.G. Park, Wrinkling of a sol-gel-derived thin film, Phys. Rev. E 71 (2005), 011604.

[61] I.Y.Y. Bu, Sol–gel production of wrinkled fluorine doped zinc oxide through hydrofluride acid, Ceram. Int. 40 (2014) 14589–14594.

[62] J.B. Miller, H.J. Hsieh, B.H. Howard, E. Broitman, Microstructural evolution of sol–gel derived ZnO thin films, Thin Solid Films 518 (2010) 6792–6798.